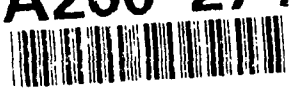

(2)

ORIENTATION PAGE

Form Approved
OMB No. 0704-0188

AGENCY USE ONLY (Leave blank)	2. REPORT DATE	3. REPORT TYPE AND DATES COVERED

4. TITLE AND SUBTITLE
Monte-Carlo Simulation of High-Field Electron Transport in Alternating-Current Thin-Film Electroluminescent Devices

5. FUNDING NUMBERS
DAAL03-91-G-0242

6. AUTHOR(S)
K. Bhattacharyya, S.M. Goodnick, J.F. Wager

7. PERFORMING ORGANIZATION NAME(S) AND ADDRESS(ES)
Oregon State University
Department of Electrical and Computer Engineering
Corvallis, OR 97331-3211

8. PERFORMING ORGANIZATION REPORT NUMBER

9. SPONSORING / MONITORING AGENCY NAME(S) AND ADDRESS(ES)
U. S. Army Research Office
P. O. Box 12211
Research Triangle Park, NC 27709-2211

10. SPONSORING / MONITORING AGENCY REPORT NUMBER
ARO 28852.3-PH

11. SUPPLEMENTARY NOTES
The view, opinions and/or findings contained in this report are those of the author(s) and should not be construed as an official Department of the Army position, policy, or decision, unless so designated by other documentation.

12a. DISTRIBUTION / AVAILABILITY STATEMENT
Approved for public release; distribution unlimited.

12b. DISTRIBUTION CODE

13. ABSTRACT *(Maximum 200 words)*

We present an ensemble Monte Carlo simulation of electron transport in bulk ZnS at high electric fields. Scattering mechanisms associated with polar optical phonons, acoustic phonons (through deformation potential coupling), intervalley scattering, and impurities (neutral and ionized) are included in a nonparabolic multi-valley model. The simulated results show that energetic electrons are available for impact excitation at fields exceeding 1 MV/cm, and that transient effects are negligible in explaining measured efficiencies in ACTFEL devices.

8pp

14. SUBJECT TERMS
ACTFEL, Electroluminescence, Monte Carlo, High-Field Transport, ZnS

15. NUMBER OF PAGES

16. PRICE CODE

17. SECURITY CLASSIFICATION OF REPORT	18. SECURITY CLASSIFICATION OF THIS PAGE	19. SECURITY CLASSIFICATION OF ABSTRACT	20. LIMITATION OF ABSTRACT
UNCLASSIFIED	UNCLASSIFIED	UNCLASSIFIED	UL

MONTE-CARLO SIMULATION OF HIGH-FIELD ELECTRON TRANSPORT IN ALTERNATING-CURRENT THIN-FILM ELECTROLUMINESCENT DEVICES

K.Bhattacharyya*, S.M.Goodnick, and J.F.Wager, *Department of Electrical and Computer Engineering, Center for Advance Material Research, Oregon State University, Corvallis,OR 97331-3211*
* On leave from the Institute of Radio Physics and Electronics, Calcutta University, Calcutta, India

ABSTRACT

We present an ensemble Monte Carlo simulation of electron transport in bulk ZnS at high electric fields. Scattering mechanisms associated with polar optical phonons, acoustic phonons (through deformation potential coupling), intervalley scattering, and impurities (neutral and ionized) are included in a nonparabolic multi-valley model. The simulated results show that energetic electrons are available for impact excitation at fields exceeding 1 MV/cm, and that transient effects are negligible in explaining measured efficiencies in ACTFEL devices.

1. *INTRODUCTION*

The operation of alternating-current thin-film electroluminescent (ACTFEL) devices depends on the physics of hot electrons in the active phosphor layer [1,2]. Currently two different views exist regarding high-field electron transport in *ZnS:Mn* ACTFEL devices based on Monte Carlo simulation. Brennan [3] performed an ensemble Monte Carlo simulation of steady state hot electron transport in bulk *ZnS* including a full band structure calculation for the density of states in the first two conduction bands and a treatment of electron-phonon scattering including collision broadening. His results have been interpreted as suggesting that very few carriers are available with sufficient energy to excite *Mn* luminescent centers in *ZnS* at fields up to 1 *MV/cm*. From this conclusion, it is difficult to explain how such high efficiencies and brightness are obtained in commercially manufactured ACTFEL devices. On the other hand, Müller and co-workers conclude [4,5] from Monte Carlo calculations and vacuum emission experiments [5] that the electrons in *ZnS* ACTFEL devices undergo *ballistic* or *loss-free* transport, resulting in extremely high energy electrons. These latter Monte Carlo calculations were performed assuming a single, parabolic conduction band with scattering assumed to occur exclusively via polar optical phonons. Furthermore, the electron distributions reported by Müller et al. [5] might be unrealistic since work by Braunlich et al. [6] indicated that the vacuum emission experiment is unreliable in assessing the high energy tail of the distribution.

We believe that high-field transport in ACTFEL devices lies in between the two extremes suggested above. The intent of the present work is to help elucidate this apparent contradiction through an investigation of transient and steady state electron transport in the active *ZnS* using an ensemble Monte Carlo simulation. A nonparabolic multi-valley model is used, including scattering due to ionized and neutral impurities, to compare the simulated hot electron distribution in ZnS to the calculated *Mn* excitation cross section [7].

2. *MONTE CARLO MODEL*

The Monte Carlo method as applied to semiconductor transport [8] is a simulation of the trajectories of individual carriers as they move through a device under the influence of external forces and subject to random scattering events. The duration of the carrier free flights between successive collisions and the scattering events involved are selected stochastically in accordance with the given transition probabilities describing the microscopic processes. In our model the conduction band is approximated by nonparabolic multi-valley (gamma, L and X) bands, with the dispersion relation

$$E(1+\alpha_n E)= \hbar^2 k^2/2m^*_n, \qquad (1)$$

where α_n, m^*_n, and k are the nonparabolicity parameter and effective mass of valley n respectively, while k is the wave vector. Between collisions, the crystal momentum changes according to the local field, while the velocity of the particle is given by

$$v = 1/\hbar\ (\partial E/\partial k). \qquad (2)$$

The duration of the free flight is given by

$$t_r = -(1/\Gamma)\ln(r), \tag{3}$$

where r is a random number uniformly distributed between 0 and 1 obtained from the computer random number generator. The total scattering rate,Γ, is given by

$$\Gamma = \Gamma_{pop} + \Gamma_{ac} + \Gamma_{iv} + \Gamma_{imp} + \Gamma_{self}, \tag{4}$$

where Γ_{pop}, Γ_{ac}, Γ_{iv}, and Γ_{imp}, are the various scattering rates considered in the present model due to polar optical phonons, acoustic phonons, intervalley scattering and impurities (both ionized and neutral) respectively. The self scattering rate, Γ_{self}, corresponds to a fictitious scattering mechanism which changes with time so that the total rate, Γ, is constant [8]. Self-scattering does not change the carrier momentum and energy, and thus does not affect the carrier's trajectory.

The scattering probability of electrons with polar optical phonons is treated assuming the Fröhlich interaction [9], while the deformation potential Ansatz is employed for acoustic and intervalley scattering. We use the Conwell and Weisskof formula [8] for ionized impurity scattering due to the small free carrier concentration in the *ZnS*. For scattering by neutral impurities (i.e. Mn^{+2}), we use Erginsoy's formula [10] which gives an energy-independent probability. The present results are obtained using the *ZnS* material parameters given by Brennan [3]. Some of the relevant valley dependent parameters are listed in the Table I.

Table I. *Valley-dependent parameters*

Parameter	gamma	L	X
Effective mass (m^*_n/m_o)	0.28	0.222	0.40
Nonparabolicity (eV^{-1})	0.690	0.650	0.360
Valley separation (eV)	...	1.449	1.454
Equivalent valleys	1	4	3

The type of scattering terminating a free flight is chosen at random according to the relative scattering rates at the end of the flight. The final angle is then chosen randomly according to the differential scattering cross section. Several thousand particles are simulated simultaneously, and ensemble averages performed to obtain the quantities of interest such as the energy, velocity, and carrier distribution function.

3. *CALCULATED RESULTS*

The scattering rates due to the various scattering mechanisms as a function of energy for the gamma valley, are shown in Fig. 1 at 300K. For the ionized impurity scattering rate shown, an impurity concentration of $1\times10^{19}/cm^3$ is used. The gamma valley scattering rate due to neutral impurities (not shown in the Fig. 1) arises from Mn doping, and is found to be approximately $10^{11}/s$ for a density of $1\times10^{20}/cm^3$. This density corresponds to 0.5 mole % doping in the cubic *ZnS*. Such a low scattering rate is found to be ineffective in affecting transport, and is neglected in most cases. As seen in Fig. 1, the gamma to X intervalley scattering rate is larger than the gamma to L rate, due to the larger X valley effective mass. Thus, the X valley is expected to be preferentially populated in comparison to L, as discussed later.

Figure 2 shows the variation of the steady state drift velocity as a function of the applied electric field for three different ionized impurity concentrations at 300 K. Brennan's [3] steady state results are included for comparison. The calculated steady-state velocity-field curve (Fig. 2) is in agreement with Brennan's results [3] at high fields but deviates from his result at low fields and is in better agreement with experimental low-field mobility

values for the *ZnS* system. The threshold field for intervalley transfer in the present study is twice that obtained by Brennen [3] which may relate to details of the band structure not included in the present model. As shown in Fig. 2, ionized impurity scattering affects the slope of the velocity-field curve for fields less than 100 *kV/cm*, and thus dominates the low field mobility for impurity densities in excess of $10^{19}/cm^3$.

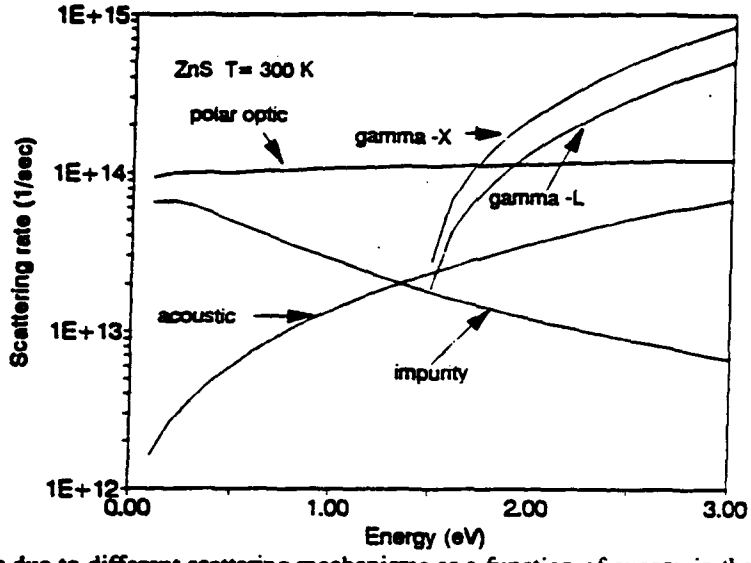

Fig. 1 Scattering rates due to different scattering mechanisms as a function of energy in the gamma valley at 300K.

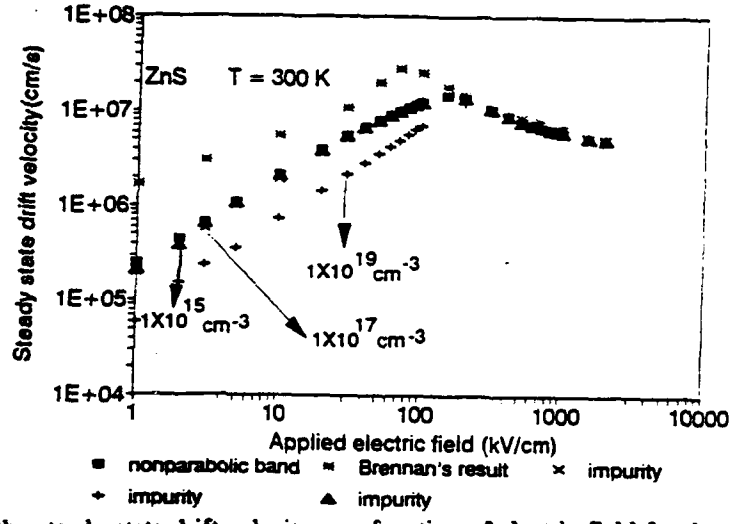

Fig. 2 Variation of the steady state drift velocity as a function of electric field for three different ionized impurity concentrations.

In Fig. 3 we plot the average velocity versus time for three different applied electric fields without ionized impurity scattering. From this figure it is clear that steady state is reached within a few tenths of a picosecond. Figure 4 gives the variation of the average electron energy with time for three different electric fields. Although there is a short time scale overshoot in the electron velocity before intervalley transfer to the L and X occurs, there appears to be no significant overshoot in the energy of the particles during the traversal time in the phosphor layer, which is approximately one to two picoseconds based on the saturated velocity at high field.

Figures 5 and 6 show the steady state electron population, $n(E)$, as a function of energy considering the total energy (kinetic plus potential) of the electrons. In Fig. 5 we plot the sum of the electron populations in the three different valleys for various electric fields. For comparison, we plot the calculated Mn impact excitation rate taken from the calculation of Shen an Xu [7] which is based on the full band structure rather than the nonparabolic model used in the Monte Carlo simulation. Fig. 6 shows the electron population in individual valleys for an electric field 2 *MV/cm*. The electron population, $n(E)$, in gamma and in X valleys is comparable (Fig.6), and much higher than

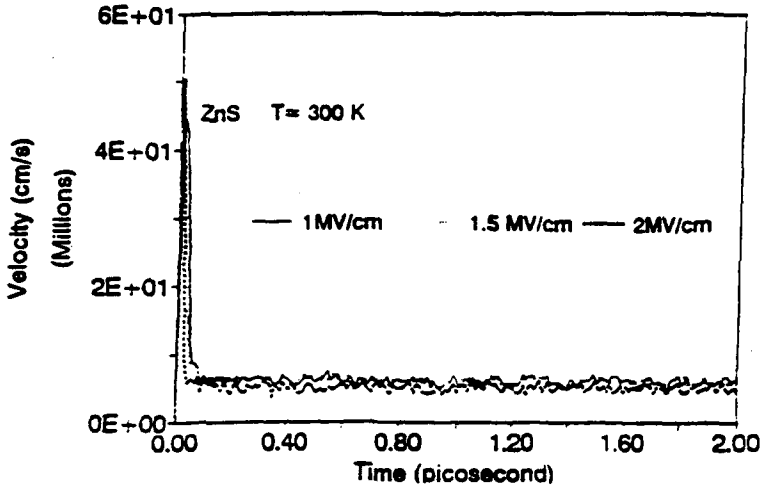

Fig. 3 Velocity versus time for three different applied electric fields without ionized impurity scattering.

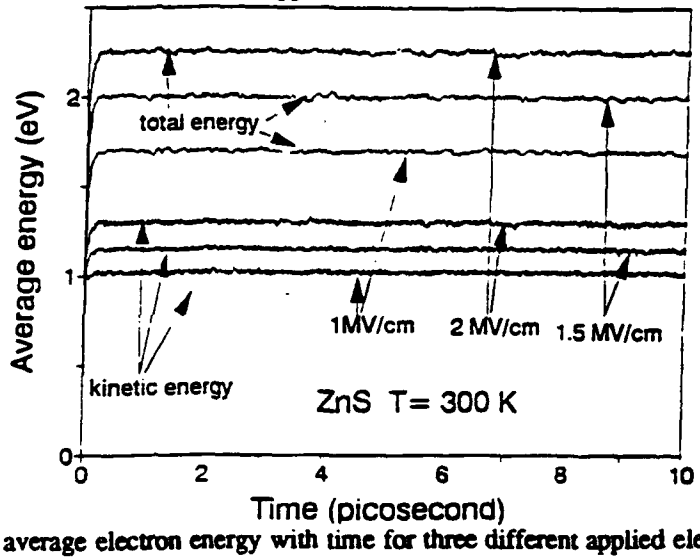

Fig. 4 Variation of the average electron energy with time for three different applied electric fields without ionized impurity scattering.

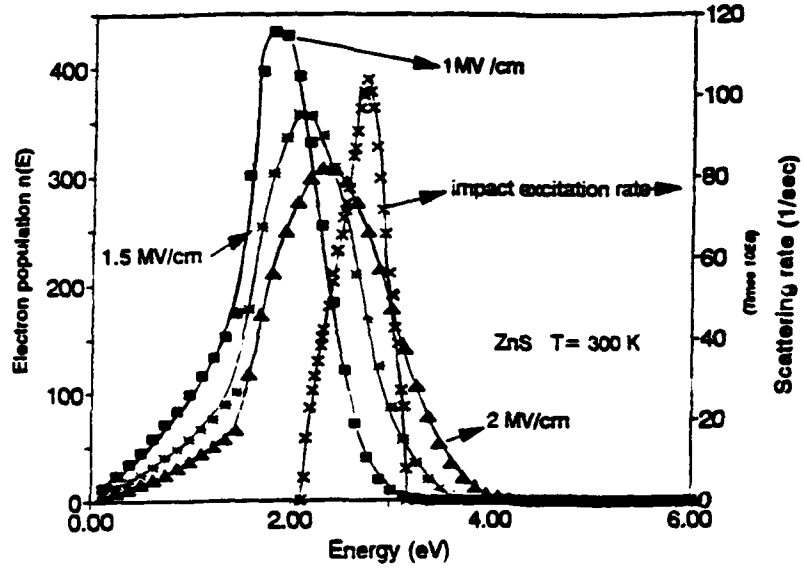

Fig. 5 The total steady state electron population, $n(E)$, and impact excitation rate, R(E), as a function of energy without ionized impurity scattering.

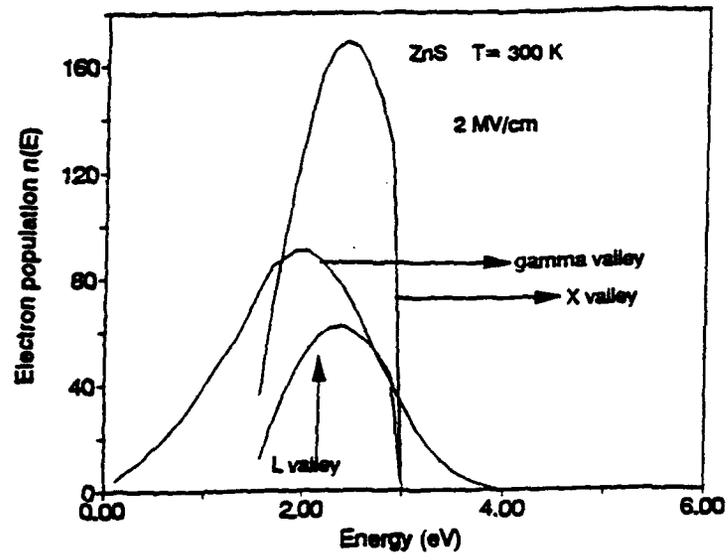

Fig. 6 The steady state electron population in three different valleys (gamma, L and X) as a function of energy without ionized impurity scattering.

that of L valley, because of the difference in intervalley scattering rates.

4. *DISCUSSION*

The material parameters used in the calculation of bulk transport are not known precisely, especially the valley dependent parameters. If we assume parabolic conduction bands, our Monte Carlo simulation exhibits electron run-away, consistent with ballistic or loss-free transport, at fields of 100 *kV/cm* and higher, in agreement with Müller and co-workers [4-5]. However, if conduction band nonparabolicity is included in the Monte Carlo simulation, we no longer observe electron run-away and the electron distribution is stable, i.e. nonparabolicity stabilizes the electron distribution by increasing the scattering rate. Furthermore, the inclusion of higher valleys and the associated intervalley scattering completely stabilizes the simulated results for all fields considered.

Ionized impurities are found to have an effect at only at low fields because the scattering rates decrease with increasing carrier energy while at high fields phonon emission increases. Thus, at the fields necessary to excite luminescence transitions, impurities play little role in the device performance. Neutral impurity scattering does not play role due to the its low scattering rate, even for densities on the order of $1\times10^{20}/cm^3$.

As seen from the Fig. 5 and 6, at fields on the order of 1 *MV/cm* and larger, a significant fraction of the total population, *n(E)*, resides at energies exceeding the threshold for luminescence excitation. Figure 5 shows that the peak of the *n(E)* versus *energy* curve shifts towards higher energy as the electric field increases from 1 *MV/cm* to 2 *MV/cm*. In comparison to the Mn excitation curve, we see a substantial overlap of the electron population which may excite transitions. This result, although obtained within an effective mass picture, is not in serious disagreement with that of Brennen [3] when normalized by the effective density of states, which is quite large at energies close to the excitation threshold. In Brennen's case [3], only the occupancy *f(E)* was shown which has led to some confusion since *f(E)* is quite small at the threshold for impact excitation. Our results show that in the field range of 1.5 to 2 *MV/cm* corresponding to the field clamping regime in *ZnS* ACTFEL devices, the *average* energy of electrons exceeds 2 *eV*, and thus there is an adequate supply of energetic carriers for efficient electroluminescence to occur.

No evidence for a significant electron population higher than 5 *eV* is found for fields up to 2 *MV/cm*, in contrast to the results of Müller and co-workers [4-5], even during the nonstationary regime. Very few carriers are available for impact ionization via electron-hole pair generation. We estimate [11,12] the threshold for band-to-band impact ionization to occur at approximately 4.3 *eV*; since Fig. 5 indicates that the high energy tail exists below approximately 4 *eV*, we do not expect band-to-band impact ionization to play an important role in the device physics of *ZnS* ACTFEL operation.

5. *CONCLUSIONS*

Monte Carlo simulation indicates polar optical phonon and intervalley scattering mechanisms to be of dominant importance, whereas neutral and ionized impurity scattering are of no significance, in determining the high field electronic transport properties of bulk *ZnS*. Nonstationary transport effects, such as velocity overshoot, are found to play no role in the operation of an ACTFEL device since the total scattering rate is found to be extremely large at the exceedingly large fields at which these devices operate. The average energy of an electron transiting a *ZnS* ACTFEL device exceeds 2 *eV* such that the electron distribution is hot enough to account for the observed efficiency of commercial ACTFEL devices. The present Monte Carlo calculations show the tail of the hot electron distribution to occur below about 4 *eV*; this would seem to preclude the occurrence of band-to-band impact ionization since this is below the 4.3 *eV* threshold energy for impact ionization.

ACKNOWLEDGEMENTS

This work was supported by the U. S. Army Research Office under contract D11L0391G0242

REFERENCES

1. J.W. Allen, J. Luminescence, **31 & 32**, 665 (1984).
2. E. Bringuier, J. Appl. Phys., **70**, 1 (1991).
3. K.Brennan, J. Appl.Phys. **64**, 4024 (1988).
4. R.Mach and G.O.Müller, J. Crys.Growth **101**, 967 (1990).
5. H.J.Fitting, G.O.Müller, R.Mach, G.U.Reinsperger, T.Hingst, and E.Schreiber, Phys. Stat.Sol.(a) **121**, 305 (1990).
6. P. Braunlich, S. C. Jones, X. A. Shen, R. T. Casper, E. Cartier, D. J. DiMaria, M. V. Fischetti, and P. Kelly, 22nd Annual Symp. on Opt. Materials for High Power Lines, Boulder, CO (1989).
7. Shen Mengyan and Xu Xurong, Solid State Commun. **72**, 803 (1989).
8. C. Jacoboni and P. Lugli, *The Monte Carlo Method for Semiconductor Device Simulation*, edited by S. Selberherr, (Springer, Wien, 1989).
9. B. R. Nag, Theory of Electrical Transport in Semiconductors, edited by B. R. Pamplin, Pergamon Press (1972).
10. C. Erginsoy, Phys. Rev. **79**, 1013 (1950).
11. C. M. Wolfe, N. Holonyak, Jr., and G. E. Stillman, Physical Properties of Semiconductors, (Prentice Hall, Englewood Cliffs, NJ, 1989), p. 299.
12. Landolt-Bornstein, New Series (Springer, Berlin, 1987), Vol. 22, pp. 167-168.